구조손상을 고려한 기설구조물의 내진성능평가

Seismic Capacity Evaluation of Existing Structures Incorporating Damage Assessment

송 종 걸[1] · 이 진 학[2] · 이 동 근[3]

Song, Jong Keol *Yi, Jin Hak* *Lee, Dong Guen*

요 약 : 이 연구는 구조물의 내진성능평가와 관련하여, 기설구조물의 현재 상태에서의 구조손상을 추정하고, 이를 반영하여 내진성능을 평가하도록 하는 절차를 제안하였다. 구조손상 추정을 위해서는 역섭동법을 사용하였고, 역섭동법의 단점을 극복하기 위하여 부분구조법과 Tikhonov의 정규화 방법을 도입하였다. 손상된 구조물의 내진성능 평가를 위하여 구조물의 지진응답과 해당 구조물의 지진손상지수를 이용하였고, 제안 방법을 20층 예제구조물에 적용하여 손상추정 결과를 반영하는 것의 영향을 분석하였다.

ABSTRACT : This paper covered two related subjects: the use of the inverse modal perturbation technique to assess structural damage in existing structures; and the use of a seismic capacity evaluation to assess damaged structures, with the aid of the identified structural damage. The substructural identification and the Tikhonov regularization algorithm were incorporated for efficient damage assessment of complex and large frame structures. The seismic capacity of a damaged structure was evaluated by comparing the structure's seismic responses and seismic damage indices. The effectiveness of the proposed method has been investigated through the numerical simulation study for a twenty-story frame structure with undamaged and damaged cases, and also different earthquake excitations.

핵 심 용 어 : 구조손상평가, 내진성능, 회전연성요구도, 지진손상지수

KEYWORDS : structural damage assessment, aseismic capacity, rotational ductility demand, seismic damage index

1. Introduction

Many existing structures designed according to older code provisions are reported to have performed poorly in recent major earthquakes such as California's 1989 Loma Prieta earthquake and 1994 Northridge earthquake, and Japan's the 1995 Kobe earthquake. Old structural systems often lack strength and ductility capacity due to the low requirements of those days and the deterioration during their service life. As a result, they are prone to severe damage or collapse during strong ground motions. Accordingly, a research on the seismic capacity evaluation that incorporates the assessment of structural damage has gradually become important to evaluate for evaluating the structural safety and for planning the retrofitting of aged structures. Similar study was carried out to investigate the seismic performance of a cantilever truss bridge using ambient vibration tests (Shama et al. 2001).

In this paper, two related theoretical backgrounds are introduced: the structural damage assessment of existing structures, and the seismic capacity evaluation. The inverse modal perturbation technique, which is a sensitivity-based method, is used to estimate the structural damage. The sensitivities of natural frequencies and mode shapes are derived from the second-order modal perturbation equations. The objective function is formulated using estimation errors in frequencies,

1) 정회원, 강원대학교 토목공학과 조교수
(Tel : 033-250-6231, Fax: 033-256-6235, E-mail : songj@kangwon.ac.kr)
2) 한국과학기술원, 스마트사회기반시설연구센터, 연구조교수, 공학박사(yijh@kaist.ac.kr)
3) 정회원, 성균관대학교 건축공학과, 교수, 공학박사(dglee@skku.ac.kr)

본 논문에 대한 토의를 2005년 4월 30일까지 학회로 보내주시면 토의 회답을 게재하겠습니다.

and the constraint equations are based on errors in mode shapes. The Tikhonov regularization algorithm (Yeo et al. 2000) is incorporated to reduce ill-posedness during inverse analysis, and the concept of substructural identification (Yun and Bhang 2000) is used for large and complex structures. In substructural identification, a structure is subdivided into several substructures and identification is carried out on one substructure at a time. This method reduces the number of required measuring points and the number of unknown structural parameters to be estimated. Eventually, the inverse analysis can be carried out in a more effective and more stable manner.

Estimating the current structural damage as a matter of course is important. However, as structural design advances toward performance- based design, information about structural performance indices such as structural seismic capacity could be much more valuable for setting up a maintenance plan for retrofitting. It can be also considered as the final goal of the structural damage detection (Rytter 1993). Seismic capacity evaluation compares seismic responses and seismic damage indices for undamaged and damaged structures. The seismic responses for those structures are evaluated as top-story displacements, base shears, rotational ductility demands and seismic energy components (Lee et al. 1997).

In general, the seismic damage index can be estimated by comparing a structure's seismic capacity and seismic demands. The rotational ductility capacity of structures as an seismic capacity was calculated using the empirical formula proposed by Daali and Korol (1996). The rotational ductility capacity for damaged structures includes the effect of the reduced stiffness. The seismic damage index for the structures subjected to the El Centro and Mexico City earthquakes was calculated using the seismic damage index proposed by Park and Ang (1985).

Numerical example study using 20-story frame was carried out to verify the proposed methods. Based on the fact that structural damage usually occurs at the bottom, several members in the bottom of the structure were assumed to be damaged in six different damage scenarios. The regularization and substructural identification were found to be very effective in identifying the structural damage for large and complex frame structures. The seismic capacity of the damaged structure is evaluated using the estimated structural damages. The importance of the seismic capacity evaluation that considers the condition of the current structural damage is verified by comparing the seismic capacities of the damaged structure (with the information about structural damage) and the undamaged structure (without the information about structural damage).

2. Theoretical Background

2.1 Inverse Modal Perturbation Technique

The initial element stiffness of the j-th member, $(EI)_j^0$, can be reduced as to $(EI)_j$ due to deterioration or any unexpected external loads such as earthquakes. Estimating the current structural conditions, a process referred to as structural damage assessment, is therefore necessary. The current element stiffness can be written using the initial element stiffness and the stiffness correction factor α_j as follows:

$$(EI)_j = \alpha_j (EI)_j^0,\ 0 < \alpha_j \leqq 1 \tag{1}$$

The severity of the structural damage severity can be determined using the reduction ratio of the element stiffness as follows:

$$d_j = 1 - \frac{(EI)_j}{(EI)_j^0} = 1 - \alpha_j,\ 0 \leqq d_j < 1 \tag{2}$$

Many techniques have been proposed for estimating the structural damage and extensive reviews can be found in the papers of Doebling et al. (1998) and others. Recently several novel damage identification techniques are developed using modal patterns (Ko et al. 2002), however, the sensitivity-based method, which is a conventional but fundamental method for estimating the structural parameters, can be useful method if remedies are incorporated to solve its peculiar shortcomings such as divergence and instability due to ill-posedness during inverse analysis (Yam et al. 2002). In this study, the inverse modal perturbation technique is used in conjunction with several enhancing techniques such as a regularization algorithm and substructural identification. This algorithm is set forth from the modal equation of a structural system.

The modal equation of the k-th mode for a structural system is written as

$$\lambda_k \boldsymbol{M}\phi_k = \boldsymbol{K}\phi_k \tag{3}$$

where $\boldsymbol{M}$ and $\boldsymbol{K}$ are the mass and stiffness matrices of an N-DOF structural system, and λ_k and ϕ_k are the eigenvalue and mode shape with N components of the k-th mode. The changes in the modal parameters $(\Delta\lambda_k, \Delta\phi_k)$ caused by changes in the stiffness properties $(\Delta\alpha_j)$ can be obtained using a second-order inverse perturbation technique. These changes are added to the prior values (λ_k, ϕ_k) and then become updated modal parameters (λ_k^*, ϕ_k^*) as:

$$\begin{aligned} \lambda_k^* &= \lambda_k + \Delta\lambda_k = \lambda_k + \sum_{j=1}^{N_{unknowns}} \lambda_{k,j}\Delta\alpha_j \\ \phi_k^* &= \phi_k + \Delta\phi_k = \phi_k + \sum_{j=1}^{N_{unknowns}} \phi_{k,j}\Delta\alpha_j \end{aligned} \tag{4}$$

where $N_{unknowns}$ is the number of unknown stiffness parameters, and $\lambda_{k,j}$ and $\phi_{k,j}$ are the sensitivities of λ_k and ϕ_k with respect to the j-th stiffness correction factor (α_j) as

$$\begin{aligned} \lambda_{k,j} &\equiv \frac{\partial\lambda_k}{\partial\alpha_j} = \frac{\phi_k^T K_{,j}\phi_k^*}{\mu_k} \\ \phi_{k,j} &\equiv \frac{\partial\phi_k}{\partial\alpha_j} = \sum_{i=1, i\neq k}^{N_{mode}} \frac{\phi_k}{\mu_i(\lambda_k^* - \lambda_i)}\phi_i^T K_{,j}\phi_k^* \end{aligned} \tag{5}$$

where μ_k is the modal mass of the k-th mode, N_{mode} is the number of considered modes, and $K_{,j}$ is the gradient matrix of K with respect to α_j. At this point, the sensitivity matrix of the mode shape $(\phi_{k,j})$ must be dimension-reduced and normalized to coincide with the measuring DOF's of the measured mode shape because the number of components of the system mode shape (N) is much more than that of the measured mode shape (N_m). Several methods have been proposed for dealing with the mode shapes that have incomplete and unmatched DOF's, though they pertain to specific structures such as a tower structural system (Feng et al. 1998). In this study, a more general formulation is proposed for handling the data with a variety of components. Consequently, the dimension reduction and the normalization of mode shape shapes should be carried out as follows:

$$\overline{\phi}_k = \frac{\boldsymbol{B}\phi_k}{|\boldsymbol{B}\phi_k|} \tag{6}$$

where $\boldsymbol{B}$ is a Boolean matrix that represents the measurement locations with $N_m \times N$ dimensions, and $\overline{\phi}_k$ is the dimension-reduced and normalized mode shape with N_m components. The updated mode shape $\overline{\phi_k^*}$ can then be obtained as follows:

$$\overline{\phi_k^*} = \overline{\phi}_k + \sum_{j=1}^{M} \overline{\phi}_{k,j}\Delta\alpha_j \tag{7}$$

where

$$\overline{\phi}_{k,j} = \frac{\boldsymbol{B}\phi_{k,j}}{\sqrt{\phi_k^T\boldsymbol{B}^T\boldsymbol{B}\phi_k}} - \frac{\phi_k^T\boldsymbol{B}^T\boldsymbol{B}\phi_k}{\sqrt{(\phi_k^T\boldsymbol{B}^T\boldsymbol{B}\phi_k)^3}}\boldsymbol{B}\phi_k$$

Hence, the updated mode shape $\overline{\phi_k^*}$ can be used to compare the updated and measured mode shapes. The Tikhonov regularization algorithm is incorporated to reduce the ill-posedness. Regularization can be achieved by adding a regularization term to the objective function that consists of estimation errors in eigenvalues. The regularization term is composed of the change in the global stiffness matrix with respect to the change of element stiffness. Finally, the objective function regarding the estimation error in the eigenvalues and the regularization term can be constructed as follows:

$$J = \sum_{k=1}^{N_{fre}} w_k \frac{(\lambda_k^m - \lambda_k^*)^2}{(\lambda_k^m)^2} + \beta\frac{\| K - K(\Delta\alpha) \|_F^2}{\| K \|_F^2}$$

subjected to

$$|\overline{\phi_{ik}^{m}} - \phi_{ik}^{*}| \leq \epsilon_k \ (1 \leq k \leq N_{mode}) \\ \alpha_{j,min} \leq \alpha_j \leq \alpha_{j,max} \ (1 \leq j \leq N_{unknown}) \tag{8}$$

where a superscript m means the measured values, w_k is a weighting factor for the k-th mode, $\Delta\alpha$ is a vector containing the N stiffness correction factors to be estimated, $\|\cdot\|_F$ represents the Frobenious norm, β is a regularization factor that can be determined by the variable regularization factor scheme, ϵ_k is an error bound that can be preset according to the measurement error in the mode shapes, and $\alpha_{j,min}$ and $\alpha_{j,max}$ are the lower and upper bounds of the stiffness correction parameter α_j.

2.2 Rotational Ductility Capacity and Seismic Damage Index

Ductility is well recognized and accepted in seismic design as a key parameter in earthquake engineering. The concept of ductility refers to the ability of a structural component or an entire structure to undergo deformation after its initial yield without any significant reduction of yield strength. In general, the inelastic behavior of structural members in nonlinear dynamic analysis is assumed to be concentrated at the end of the members. Accordingly, rotational ductility can be a useful parameter for evaluating seismic capacity. The rotational ductility capacity can be estimated by the ratio of the maximum rotation at the end of a member under monotonic loading to the yield rotation. The rotational ductility capacity is not easily predicted by analytical tools. An empirical expression developed by Daali and Korol (1996) from experimental test results on a rolled I-section steel beam is used. The rotational ductility capacity is given by

$$\mu_{capacity} = 1 - 9.2\lambda + 10.71\lambda^{-0.293} \\ \lambda = \frac{\alpha_f \alpha_w \alpha_l}{30072}, \alpha_f = \frac{b}{t\epsilon}, \alpha_w = \frac{d}{w\epsilon}, \alpha_l = \frac{L}{r_y \epsilon}, \epsilon = \left(\frac{300}{\sigma_y}\right)^{1/2} \tag{9}$$

where b is the half-section width, t is the flange thickness, d is the clear section depth between flanges, w is the web thickness, L is the distance between the lateral support and the point of the maximum moment, and r_y is the radius of gyration around the weak axis and σ_y is the yield stress. The numerator within the square root is expressed in MPa.

The damage parameters reflect a realistic damage process of the structures subjected to earthquake loads, and the values can be evaluated easily and accurately. The ductility demand and the hysteretic energy have been widely used as damage parameters. In this study, the damage index proposed by Park and Ang (Park and Ang (1985) is used for seismic damage analysis. Park and Ang's damage index (D_{PA}) is defined as a linear combination of the ductility demand (or the maximum displacement) and the dissipated hysteresis energy. The damage index is defined as

$$D_{PA} = \frac{x_{max}}{x_{u,mon}} + \beta\frac{E_h}{F_y x_{u,mon}} = \frac{\mu + \beta(\mu_e - 1)}{\mu_{u,mon}} \\ \mu_e = \frac{E_h}{F_y x_y} + 1 \tag{10}$$

where x_{max} is the maximum displacement, $x_{u,mon}$ is the allowable value of the maximum displacement, E_h is the dissipated hysteresis energy, F_y is the yield force and β is the calibration factor which represents the structural degradation and is in the range of -0.3 ~ 1.2. In this study, a value of 0.15 is used for β because 0.15 is the mean value of the experimental results (Uang 1991). The parameter μ is the ductility demand defined as the ratio of the maximum displacement x_{max} to the yield displacement x_y, while μ_e is the hysteresis ductility, and $\mu_{u,mon}$ is the maximum allowable value of ductility. In this study, $\mu_{u,mon}$ is equal to the rotational ductility capacity.

Noticeably, the damage index is not normalized; that is, the damage index is not 0 when $x_{max} = x_y$, and is not 1 in the case of failure under monotonic loading. Therefore, in this study, if the maximum displacement of a structure does not exceed the yield displacement, the damage index is assumed to have a value of zero.

3. Numerical Verification

3.1 Example Structure

For the example study, a twenty-story frame structure shown in Figure 1 were used. The section profiles and the member ID's are shown in Table 1 and Figure 1 (Roedar et al. 1993). This structure is designed according to the concept of the strong-column and weak-beam (SCWB) system. This concept is popularly used in the design of general steel frame structures. The material properties for the structure are assumed to be 20 GPa for an elastic modulus and 8000 kg for the lumped mass of each story. The elastic modulus is the value of steel, and the lumped mass is based on the slab and other nonstructural members.

The lower four natural frequencies of the structure are 0.342Hz, 0.966Hz, 1.697Hz, and 2.418Hz, and the mode shapes for the lower three modes are shown in Figure 2.

Table 1. Sections for example structures

ID	Interior Columns	Exterior Columns	ID	Girders
C10	W27X84	W14X74	B10	W24X62
C9	W27X102	W14X90	B9	W24X68
C8	W30X116	W14X109	B8	W24X76
C7	W30X132	W14X120	B7	W24X76
C6	W36X135	W14X132	B6	W27X84
C5	W36X150	W14X145	B5	W27X84
C4	W36X160	W14X159	B4	W27X94
C3	W36X170	W14X176	B3	W27X94
C2	W36X182	W14X193	B2	W27X102
C1	W36X232	W14X211	B1	W27X102

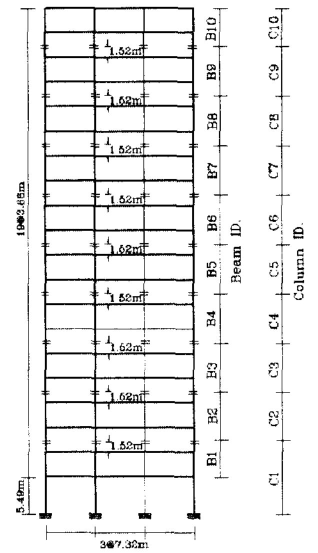

Figure 1. Member ID of example structures

(a) Mode 1 (b) Mode 2 (3) Mode 3

Figure 2. Mode shapes of example structure

In six damage scenarios, the structural damage is assumed to occur only in the bottom at two girder members (Gm2 and Gm9 in Figure 3) and one column member (Cm2 in Figure 3). The inflicted damage scenarios are listed in Table 2, and the natural frequencies for the lower four modes at the damage scenarios are summarized in Table 3.

Table 2. Damage scenarios

Damage Cases	Gm2	Gm9	Cm2
Case 1	-20%	-	-
Case 2	-30%	-15%	-
Case 3	-30%	-30%	-
Case 4	-	-	-20%
Case 5	-30%	-	-20%
Case 6	-30%	-20%	-20%

Table 3. Natural frequencies

Cases	Mode 1	Mode 2	Mode 3	Mode 4
Undamaged	0.342	0.966	1.697	2.418
Case 1	0.341	0.964	1.694	2.417
Case 2	0.341	0.962	1.692	2.415
Case 3	0.340	0.960	1.691	2.414
Case 4	0.342	0.964	1.694	2.416
Case 5	0.341	0.961	1.689	2.410
Case 6	0.340	0.959	1.687	2.409

As shown in Figure 3, only 12 points could be measured at once in the example structure: three horizontal components and nine vertical components in the lower parts of the structure. The possibility of such a measurement is based on the assumption that the inspection for that part is more crucial. Furthermore, only 13 members, comprising four column members (Cm1~Cm4) and nine girder members (Gm1~Gm9), were estimated by using substructural identification, which makes the damage estimation more efficient and stable. If this technique is not used, many more measuring points are required. Moreover, the number of unknown parameters might become very large insolvably. If a three-dimensional approach is carried out, the problem could become much more severe.

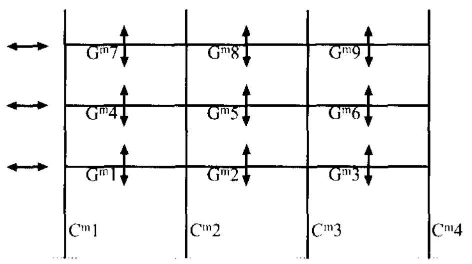

Figure 3. Measuring points and unknown members

3.2 Structural Damage Assessment

The natural frequencies for lower four modes and the mode shapes for lower three modes are used to estimate the structural damages. The severity of the estimated damage is shown in Figure 4. The structural damages for the cases 1 to 4 were more accurately estimated than those for the cases 5 and 6.

Structural damage at certain members can affect the global behavior of a structure. The behavior of a structure can be significantly different because of a damaged member. However, as a structure becomes more complex, the effect of structural damage at an individual member is limited to adjacent members; the damage does not affect the whole structure. If structural damage causes the whole structure to collapse or has a significant effect, the design can be considered as non-redundant or badly worked, because today's structures should have a sufficient number of redundancies to prevent a catastrophic incident. Naturally, a slight change occurs in the behavior of the whole structure, but it is likely to be very small; often it is unnoticeable.

Structural damage at a certain member can affect the adjacent member's behavior. Therefore, structural damage can be evaluated if a sufficient number of sensors are installed at certain locations in a region, including the damaged member. The estimated results are worse for damage cases 5 and 6 than for the other cases because the damaged members affect the local behavior of the structure in a more complicated way whenever two or three members of in a local region are damaged. Consequently, additional sensors are needed for a more exact estimation, though a smaller number of sensors is more desirable. Nonetheless, the estimated severity of damage for the healthy members ($d_j = 0$) seems to be less significant, that is, only a few false alarming alarm errors occur. In conclusion, the structural damage estimation performed quite well, and the damaged members were successfully located using an inverse modal perturbation technique in conjunction with regularization and substructuring concepts.

This conclusion, however, is not sufficient to determine a pertinent maintenance plan for retrofitting because the reduction of the structural stiffness does not directly mean the lack of structural performance in seismic capacity. To do the complementary work, the estimated current structural conditions are used to successively evaluate the seismic capacity of damaged structure.

3.3 Nonlinear Time Domain Analyses

Seismic responses were computed for the example structure with and without damage. The stiffness reductions were assigned as 30% for the Gm2 girder, as 20% for the Gm9 girder, and as 20% for the Cm2 column (Damage Case 6).

Two earthquake records were selected for this study: the NS component of the 1940 El Centro earthquake and the EW component of the 1985 Mexico City earthquake. To get an effective peak acceleration (EPA) of 0.4 g for 5 percent of the critical damping ratio, 0.5g was selected as the peak ground acceleration of the El Centro earthquake and 0.25g was selected for Mexico City earthquake. The scaled acceleration records are shown in Figures 5(a) and 5(b). Spectral acceleration in the range of 0.1 sec ~ 0.5 sec was used to evaluate the EPA for the El Centro earthquake, while spectral acceleration in the range of 1 sec ~ 5 sec was used to determine the EPA for the Mexico City earthquake record.

The seismic responses of the structures with and without damage are presented in terms of top-story displacement, base shear and hysteretic energy of the system-level. Here, the results of selected responses are discussed, since the other results have similar trends. In Figures 6, the top-story displacement and base shear are compared for the structure subjected to Mexico City earthquake with and without damage. The responses of the structure with and without damage are very similar. In Figure 7, the hysteretic energy components are compared with and without damage. This result shows that the hysteretic energy components of the structure with damage are slightly larger than those of the structure without damage. The difference of the hysteretic energy for the structure with and without damages is reduced with increasing the number of structural members (or redundancies). Overall, the difference of the seismic response owing to the damaged members is not distinguished clearly for the whole structural system. Therefore, the comparison of seismic responses for the member-level may present more important information for the evaluation of the seismic capacity.

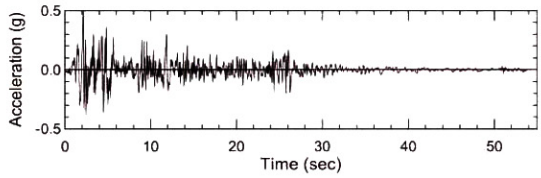

(a) El Centro earthquake (NS, 1940)

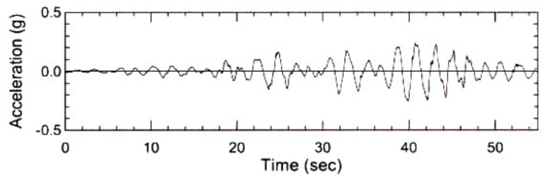

(b) Mexico City earthquake (EW, 1985)

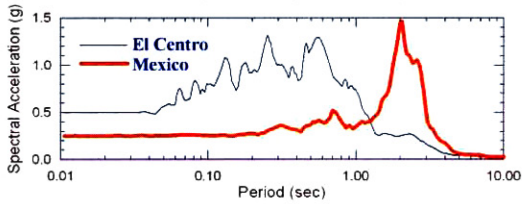

(c) Response spectra for 5% damping ratio

Figure 5. Input ground acceleration (scaled EPA= 0.4 g)

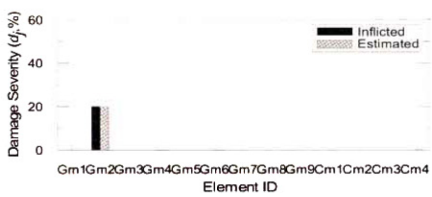

(a) Damage Case 1

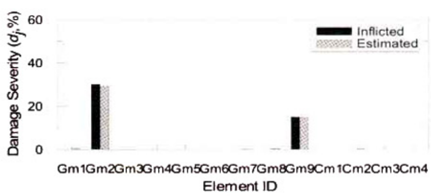

(b) Damage Case 2

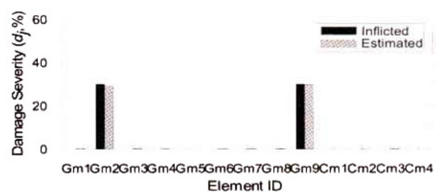

(c) Damage Case 3

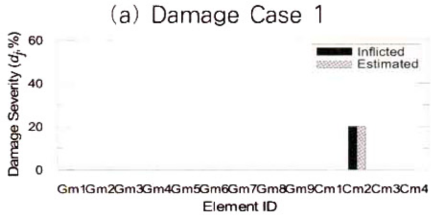

(d) Damage Case 4

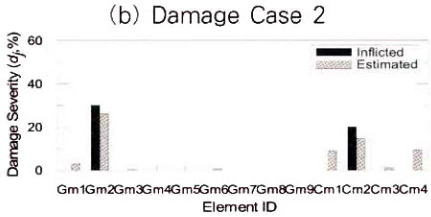

(e) Damage Case 5

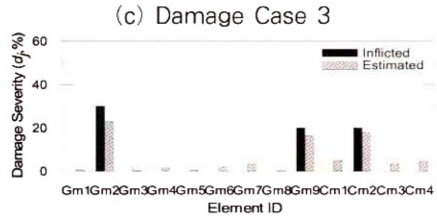

(f) Damage Case 6

Figure 4. Damage estimation result for frame SCWB20

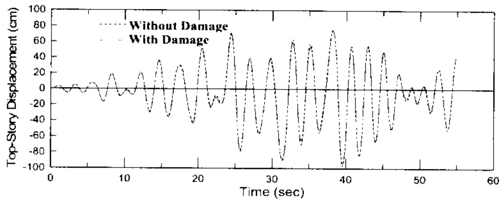

(a) Top story displacement

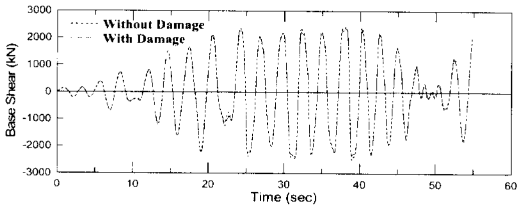

(b) Base Shear

Figure 6. Seismic responses for example structure subjected to Mexico earthquake(Damage Case 6)

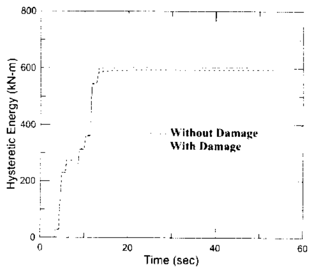

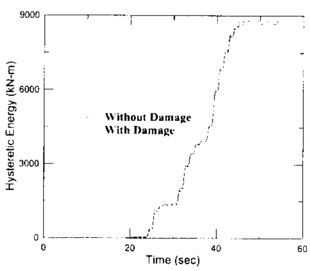

(a) El Centro 지진 (b) Mexico 지진

Figure 7. Comparison of hysteretic energy (Damage Case 6)

3.4 Evaluation of Rotational Ductility Capacity

The rotational ductility capacity should be used as an important parameter for seismic damage analysis of structural members. Figure 8 compares the rotational ductility capacities that were estimated for the example structure, with and without damage, by using Equation (9). In this figure, circles depict the relative magnitudes of the capacities, and the magnitude of base circle is shown in the bottom and right side of each figure. Because the example structure is designed by the SCWB design concept, the trend of the calculated rotational ductility capacity coincides with the SCWB concept. Generally, for properly designed structure, the lower the story, the larger the size of the members; and the larger the size of the members; the higher the rotational ductility capacity.

The effect of reduced stiffness for the rotational ductility capacity is summarized in Table 4. The rotational ductility capacities of the damaged members are reduced in the range of 68~89 percent of those of the undamaged members.

Table 4. The effect of damage for ductility capacity

Member ID	Rotational Ductility Capacity	
	without Damage	with Damage
Gm2	9.9	6.7
Gm9	9.9	7.9
Cm2	18.3	16.8

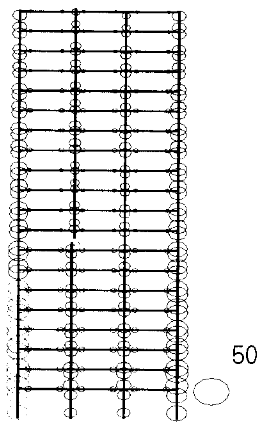

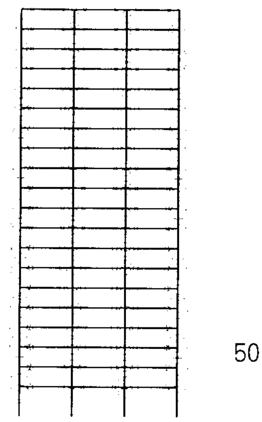

(a) without damage (b) with damage

Figure 8. Comparison of rotational ductility capacity

3.5 Seismic Damage Analysis

The level of risk associated with the loss of serviceability, severe damage, or collapse of existing structures can be evaluated by the seismic damage analysis. With this risk quantified, rational decisions can be made as to whether the structure should be retrofitted or replaced.

The rotational ductility and the hysteretic energy demands used as the components of the seismic demand in the seismic damage analysis are shown in Figures 9 and 10. In these figures, the relative magnitudes of each demand are depicted by circles. From the comparison with the inelastic responses of the undamaged and damaged structures, it can be shown that the concentration of the inelastic responses on the damaged members is not significant due to the moment redistribution induced by many adjacent members. On the contrary, inelastic responses are concentrated on the adjacent members than the damaged members. Particularly, the hysteretic energy demands are more concentrated on the adjacent members than the rotational ductility demands. These trends may be explained by noting that the reduction of the yield moment that resulted from the reduced stiffness caused a reduction in the capacity of the hysteretic energy dissipation. Also, it may be additionally explained that the rotational ductility demand is the maximum inelastic response, while the hysteretic energy demand is the cumulative inelastic response.

The seismic damage indices are estimated from the rotational ductility capacity shown in Figure 9 and the seismic demands such as the rotational ductility and the hysteretic energy demands shown in Figures 9 and 10. The estimated damage indices are shown in Figure 11. The damage indices for Mexico City earthquake are larger than those for El Centro earthquake. The main reason of this trend can be explained that the primary period (about 2 second) corresponding to the maximum spectral acceleration of Mexico City record shown in Figure 5(c) is more close to the fundamental periods of the example structure than that of El Centro record. Although the inelastic responses are more concentrated on the adjacent members than the damaged members, the damage indices of the damaged members are significantly larger than the adjacent members, since the rotational ductility capacity in the case of the damaged members is reduced. Therefore, in the case of the estimation of the seismic damage index, the influence of the reduced rotational ductility capacity may be more dominant than the concentration influence of seismic demands.

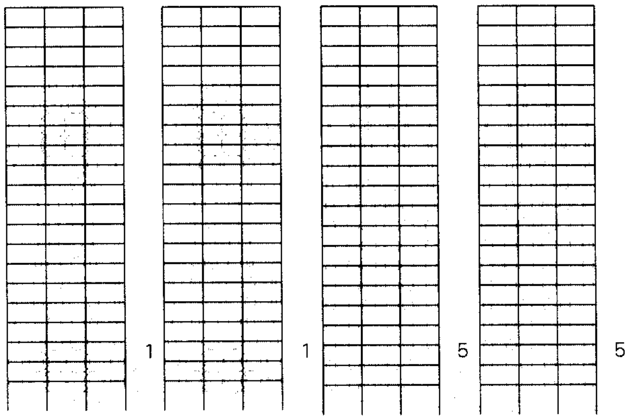

(a) El Centro w/o damage (b) El Centro w/ Damage (c) Mexico w/o damage (d) Mexico w/ damage

Figure 9. Comparison of rotational ductility demands

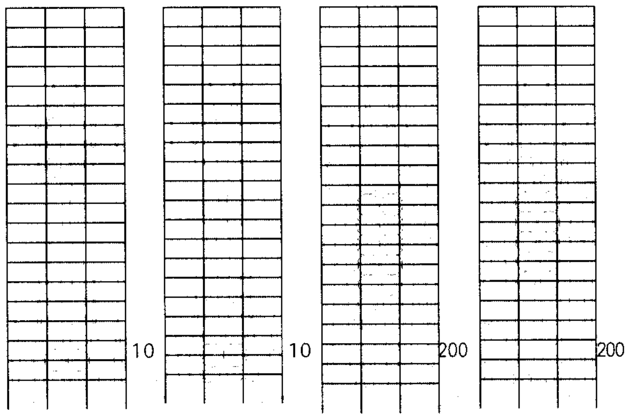

(a) El Centro w/o damage (b) El Centro w/ Damage (c) Mexico w/o damage (d) Mexico w/ damage

Figure 10. Comparison of hysteretic energy (unit:kN-m)

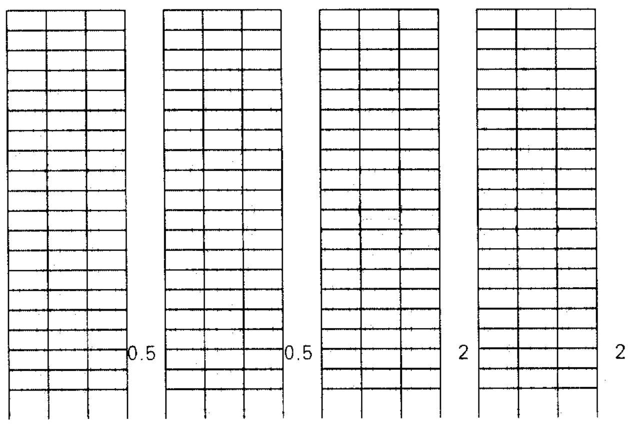

(a) El Centro w/o damage (b) El Centro w/ Damage (c) Mexico w/o damage (d) Mexico w/ damage

Figure 11. Comparison of damage index

4. Conclusion

Based on the damage assessment and seismic capacity evaluation, the following main conclusions can be drawn:

(a) For a more efficient and stable damage assessment, substructural identification and a regularization algorithm are incorporated into a conventional damage assessment technique. Structural damage can be estimated with negligible errors if a single member is damaged or two members not closely located are damaged. Structural damage with two or three damaged locations were can be reasonably estimated with only a few false alarm errors, though the errors are insignificant.

(b) For the aseismic capacity evaluation, the seismic responses and the seismic damage indices for the undamaged and damaged structures are compared. To estimate the seismic damage indices, the rotational ductility capacities are calculated by the empirical formula. The overall trends of the calculated rotational ductility capacities are comparable with the design strength distributions. From the seismic responses of the damaged structures, it can be shown that the inelastic responses are more concentrated on the adjacent members than the damaged members. The influence of the reduced rotational ductility capacity may be more dominant than the concentration influence of seismic demands in the case of the estimation of the seismic damage index for the damaged members.

Acknowledgement

This study was carried out under the financial support from Smart Infra-Structure Technology Center (SISTeC) under the sponsorship from Ministry of Science and Technology (MOST) and Korea Foundation of Science and Technology (KOSEF).

References

Daali M.L., Korol R.M. (1996) Adequate ductility in steel beams under earthquake-type loading. *Engineering Structures* Vol. 18, No. 2, pp. 179-189.

Doebling S.W., Farrar C.R., Prime M.B. (1998) A summary review of vibration-based damage identification methods. The Shock and Vibration, Diegest. Vol. 30, No. 2, pp. 91-105.

Feng M., Kim J.M., Xue H. (1998) Identification of a dynamic system using ambient vibration measurement. *Journal of Applied Mechanics ASME*. Vol. 65, No. 4, pp. 1010-1021.

Ko J.M., Sun Z.G., Ni Y.Q. (2002) Multi-stage identification scheme for detecting damage in cable-stayed Kap Shui Mun bridge. *Engineering Structures* Vol. 24, pp. 857-868.

Lee D-G., Song J-K., Yun C-B. (1997) Estimation of system level ductility demands for multi-story structures. *Engineering Structures* Vol. 19, No. 12, pp. 1025-1035.

Park Y.J., Ang A-H.S. (1985) Mechanistic seismic damage model for reinforced concrete. *Journal of Structural Engineering, ASCE*, Vol. 111, pp. 722-739.

Roeder C.W., Schneider S.P., Carpenter J.E. (1993) Seismic behavior of moment-resisting steel frames: analytical study. *Journal of Structural Engineering ASCE*. Vol. 119, No. 6, pp. 1866-1884.

Rytter A., (1993) Vibration based inspection of civil engineering structures. PhD thesis, Department of Building Technology and Structural Engineering, Aalborg University, Denmark.

Shama A.A., Mander J.B., Chen S.S., Aref A.J. (2001) Ambient vibration and seismic evaluation of a cantilever truss bridge. *Engineering Structures*, Vol. 23, pp. 1281-1292.

Uang, C.M. (1991) Establishing R(or R_w) and C_d factors for building seismic provisions, *Journal of Structural Engineering, ASCE*, Vol. 117, No. 1, pp. 19-28.

Yam L.H., Li Y.Y., Wong W.O. (2002) Sensitivity studies of parameters for damage detection of plate-like structures using static and dynamic approaches. *Engineering Structures* Vol. 24, pp. 1465-1475.

Yeo I.H., Shin S.B., Lee H.S., Chang S.P. (2000) Statistical damage assessment of framed structures from static response. *Journal of Engineering Mechanics, ASCE,* Vol. 126, No. 4, pp. 414-421.

Yun C-B., Bahng E.Y. (2000) Substructural identification using neural networks. Computers and Structures, Vol. 77, pp. 41-52.

(접수일자 : 2004. 7. 8 / 심사일 2004. 7. 23 / 심사완료일 2004. 8. 27)